Foxj1 regulates basal body anchoring to the cytoskeleton of ciliated pulmonary epithelial cells

Brigitte N. Gomperts, Xiulan Gong-Cooper and Brian P. Hackett*

Developmental Biology Research Unit, The Edward R. Mallinckrodt Department of Pediatrics, Washington University School of Medicine, St Louis, MO 63110, USA

*Author for correspondence (e-mail: hackett@kids.wustl.edu)

Accepted 11 November 2003
Journal of Cell Science 117, 1329-1337 Published by The Company of Biologists 2004
doi:10.1242/jcs.00978

Summary

The forkhead box transcription factor Foxj1 is required for cilia formation and left-right axis determination. To define the role of Foxj1 in ciliogenesis, microarray analysis was performed to identify differentially expressed genes in the pulmonary epithelium of *foxj1*$^{+/+}$ and *foxj1*$^{-/-}$ mice. In the absence of Foxj1, the expression of calpastatin, an inhibitor of the protease calpain, decreased. RNase protection confirmed the decrease in calpastatin expression and decreased calpastatin was detected in the proximal pulmonary epithelium of *foxj1*$^{-/-}$ mice by immunohistochemistry. No change was detected in the expression of calpain 2 in the pulmonary epithelium by western blot or immunohistochemistry. By western blot and immunofluorescence, ezrin, a substrate for calpain, was also found to decrease in the pulmonary epithelium of *foxj1*$^{-/-}$ mice. No change in ezrin gene expression was found by RT-PCR. A decrease in ezrin binding phosphoprotein-50 (EBP-50) was also detected by immunofluorescence in the *foxj1*$^{-/-}$ mouse pulmonary epithelium. Immunoelectron microscopy demonstrated ezrin associated with the basal bodies of cilia in the pulmonary epithelium. Treatment of tracheal explants from *foxj1*$^{-/-}$ mice with a calpain inhibitor resulted in a partial reappearance of cilia observed in these mice. Additionally, following treatment of *foxj1*$^{-/-}$ tracheal explants with calpain inhibitor, basal bodies were observed in an apical location along with relocalization of ezrin and EBP-50. Regulation of calpain activity by calpastatin thus provides a mechanism for regulating the anchoring of basal bodies to the apical cytoskeleton in ciliated cells. In the absence of Foxj1, decreased calpastatin expression with decreased ezrin and EBP-50 results in an inability of basal bodies to anchor to the apical cytoskeleton and subsequent failure of axonemal formation.

Key words: foxj1, Calpastatin, Calpain, Ezrin, Cilia, Basal body

Introduction

Mucociliary clearance is an important component of the innate host defense of the pulmonary system. Cilia, in conjunction with secreted mucus, provide a mechanism for the removal of infectious or other potentially injurious substances from the lung. Ciliary motility and the characteristics of the airway surface liquid are crucial to the maintenance of this defense (Knowles and Boucher, 2002). The importance of this protective mechanism in the lung is demonstrated by individuals with the immotile cilia syndrome. The absence of normal ciliary motility in these patients is associated with recurrent pulmonary infections that may ultimately result in chronic pulmonary disease characterized by bronchiectasis with associated obstructive and/or restrictive lung disease (Afzelius and Mossberg, 1995). The immotile cilia syndrome has been linked to multiple genetic loci and recently some of the genes mutated in this syndrome have been identified (Guichard et al., 2001; Olbrich et al., 2002; Pennarun et al., 1999). Another example of the importance of this defense is in cystic fibrosis where abnormal ion and water transport across the pulmonary epithelium results in altered airway surface liquid and defective mucociliary clearance (Knowles and Boucher, 2002). In addition to these genetic causes, abnormal mucociliary clearance may be seen in association with lung infections, asthma and other pulmonary diseases (Salathe et al., 1997). The loss of normal mucociliary clearance is an important component of the pathophysiology of these pulmonary diseases. Whether there is subsequent recovery of normal clearance or not may play an important role in the long-term outcome of these diseases. Despite the importance of cilia to the innate defense of the lung, the molecular and cellular mechanisms regulating cilia formation and stability remain largely unknown.

The axonemes of the cilia typically found in the vertebrate respiratory, reproductive and central nervous systems are characterized by nine microtubule pairs surrounding a central pair (referred to as 9+2). Dynein arms connect adjacent microtubule pairs and provide an ATPase activity required for motility. The axoneme is anchored to the apical surface of the cell through a basal body that also serves as a template for axonemal assembly (Preble et al., 2000). Basal bodies are formed in the cytoplasm of cells and transported to the cell apex where axonemal assembly occurs (Dirksen, 1991; Sorokin, 1968). The complexity of axonemal and basal body structure is underscored by the estimate that more than 250 different proteins are required for the formation of eucaryotic cilia and flagella (Dutcher, 1995). Much of the current understanding of the mechanisms regulating cilia and flagella

formation has come from the study of mutations that disrupt assembly of axonemes in flagellate, unicellular organisms such as *Chlamydomonas* (Tam and Lefebvre, 1993). Vertebrate homologues for some of these genes have been identified and shown to also be required for cilia assembly in vertebrates (Cole et al., 1998; Marszalek et al., 1999; Nonaka et al., 1998; Takeda et al., 1999).

Foxj1 (formerly HFH-4) is a member of the forkhead box family of transcription factors that are characterized by a conserved 100 amino acid DNA binding domain (Hackett et al., 1995). Foxj1 is expressed in ciliated cells of the respiratory, reproductive and central nervous systems (Blatt et al., 1999; Hackett et al., 1995; Lim et al., 1997; Pelletier et al., 1998; Tichelaar et al., 1999). Targeted mutation of the mouse *foxj1* gene results in an absence of 9+2 axonemal structures and a failure of normal localization of basal bodies to the apices of cells (Brody et al., 2000; Chen et al., 1998). Additionally, homozygous mutant mice demonstrate random determination of left-right axis asymmetry (Chen et al., 1998). The defect in cilia formation in mice lacking Foxj1 has not been defined but the cytoplasmic location of basal bodies in the homozygous mutant mice suggests a defect in basal body transport or anchoring to the apical cytoskeleton. Although a number of basal body-associated proteins have been described, the mechanisms regulating transport and anchoring of basal bodies to the cell apex remain unknown (Geimer et al., 1998; Lechtreck et al., 1999; Silflow et al., 2001; Taulman et al., 2001). In this report, regulation of basal body anchoring to the apical cytoskeleton by Foxj1 is described.

Materials and Methods

Experimental animals

Mice with a targeted mutation of the *foxj1* gene were generated as described previously (Chen et al., 1998). Homozygous mutant animals were obtained by mating $foxj1^{+/-}$ male and female mice. Genotyping was performed as described previously (Chen et al., 1998). All animal experiments were approved by the Washington University School of Medicine Animal Studies Committee in accordance with NIH guidelines for animal care and use.

DNA microarray analysis

Total RNA was isolated from embryonic day (E) 15.5 $foxj1^{+/+}$ and $foxj1^{-/-}$ lung tissue using TRIzol (Invitrogen) extraction and ethanol precipitation. The preparation and labeling of targets for Affymetrix GeneChip Mu74A analysis was performed at the Multiplexed Gene Analysis Core Facility of the Siteman Cancer Center at Washington University School of Medicine according to the manufacturer's protocols. Separate Mu74A GeneChips were hybridized with targets generated from $foxj1^{+/+}$ and $foxj1^{-/-}$ E15.5 pooled lung RNA. Hybridizations were performed in triplicate. Following hybridization, probe arrays were washed, stained and scanned with a Hewlett Packard GeneArray Scanner. Data were analyzed and comparison of gene expression levels between $foxj1^{+/+}$ and $foxj1^{-/-}$ lung tissue made with Affymetrix software.

Ribonuclease protection assay

Oligonucleotide primers to the 5′ region of the calpastatin cDNA were generated based on the mouse calpastatin sequence (GeneBank accession number AB026997): 5′-ATGTCCCAGCCCGGCCCAAG-3′ and 5′-CCTCTGCTGCCACCAGCAAGT-3′. A 250 base pair calpastatin fragment was amplified from E15.5 lung total RNA by RT-PCR and subcloned into the pCR II plasmid vector (Invitrogen). Antisense calpastatin and [^{32}P]GAPDH cRNA probes were synthesized by in vitro transcription. RNase protection assays were performed with the RPA III kit (Ambion). Probes were hybridized overnight at 42°C with 10 μg of total RNA. Single stranded RNA was digested with RNaseA/RNaseT1 and samples electrophoresed in 6.0% polyacrylamide-urea and autoradiography performed. Bands corresponding to protected fragments were quantified with a Molecular Dynamics Phosphoimager and Storm Scanner. A GAPDH protected fragment was used as a loading control. RNase protection assays were performed in triplicate with independent RNA samples.

Western blot analysis

Protein was isolated from E15.5 $foxj1^{+/+}$ and $foxj1^{-/-}$ mouse lung tissue in the presence of protease inhibitors as described previously (Potter et al., 1998). 10 μg of the cytoplasmic protein fraction was electrophoresed in 7.0% polyacrylamide-SDS and transferred to a PVDF membrane (Amersham). The membrane was blocked for 1 hour at room temperature with 5.0% (w/v) nonfat dry milk in Tris-buffered saline with 0.1% (v/v) Tween 20. Primary antibodies used were murine monoclonal anti-bovine calpastatin (1:2000; Sigma), rabbit anti-human recombinant calpain 2 (1:1000; Triplepoint Biologics), rabbit polyclonal anti-human ezrin (1:2000; Upstate Biotechnology) and murine monoclonal anti-rabbit GAPDH (1:5000; Research Diagnostics). Secondary antibodies were either anti-mouse or anti-rabbit IgG antibody linked to horseradish peroxidase (Amersham). A chemiluminescent signal was generated with ECF or ECL Plus (Amersham) and quantified with a Molecular Dynamics Phosphoimager and Storm Scanner. GAPDH was used as a loading control for standardization of blots. Western blot analysis was performed in triplicate.

Immunohistochemistry and immunofluorescence

Lung tissue was fixed in 10% (v/v) buffered formalin for 72 hours at 4°C, dehydrated in ethanol, paraffin wax embedded, and sectioned. Antigen unmasking was performed by heating sections in Antigen Unmasking Solution (Vector Laboratories) to boiling for 6 minutes in a microwave oven. Endogenous peroxidase activity was quenched with 0.1% (v/v) hydrogen peroxide and sections blocked with appropriate animal sera for 30 minutes. Primary antibodies were: murine monoclonal anti-bovine calpastatin (1:500; Sigma), rabbit anti-human recombinant calpain 2 (1:250; Triplepoint Biologics), rabbit polyclonal anti-human ezrin (1:100; Upstate Biotechnology), polyclonal anti-EBP-50 (1:100; ABR), and mouse monoclonal anti-acetylated α-tubulin (1:500; Sigma). After incubation with primary antibody for 1 hour, sections were incubated with biotinylated secondary antibodies for 30 minutes. Immunoperoxidase staining was performed with a Vectastain ABC kit (Vector Laboratories) and Vector NovaRed peroxidase substrate (Vector Laboratories). Sections were counterstained with Hematoxylin and nuclei blued with 0.7% (v/v) NH_4OH.

For sequential, double immunofluorescence, blocking serum was applied for 20 minutes followed by incubation with the first primary antibody at 4°C overnight. The appropriate biotinylated secondary antibody (Vector) was then applied to the sections for 45 minutes at room temperature and then incubated with fluoroscein avidin D or rhodamine avidin D for 30 minutes. Following blocking with an avidin/biotin blocking reagent (Vector), sections were incubated with the second primary antibody at 4°C overnight. Sections were then incubated for 45 minutes with the appropriate biotinylated secondary antibody and then with fluoroscein avidin D or rhodamine avidin D.

For immunohistochemistry and immunofluorescence, a minimum of three independent sections from wild-type or mutant lung tissue was examined. Duplicate samples were included for each antibody and tissue as well as control samples with no primary antibody.

Reverse transcriptase polymerase chain reaction (RT-PCR)

SuperScript reverse transcriptase (Gibco-BRL) was used for first strand cDNA synthesis from total lung RNA with random hexamers. Gene-specific PCR amplification was performed for 25 cycles with denaturing at 94°C for 30 seconds, annealing at 58°C for 30 seconds, and elongation at 72°C for 2 minutes. Gene-specific primers were: 5′-GAAGGTGGCATGGAGGAGCCG-3′ and 5′-TGGGTTGGTG-GCATAGTCCAC-3′ for Foxj1; 5′-AGCGACAGCAGTTGG-GAAGCC-3′ and 5′-CAGTTGGAGGGCCTTCTCAAT-3′ for ezrin and 5′-AAATTTTCAAAGCTCAGTCTG-3′ 5′-AAAATCTGCT-GAAAGCTCCCC-3′ for calpastatin. Amplification of β-actin was performed as a positive control. For all samples, controls without reverse transcriptase were included to exclude amplification from genomic DNA.

Electron microscopy

For transmission electron microscopy, tracheal tissues were fixed with 2.5% (v/v) glutaraldehyde in 0.1 M sodium cacodylate, postfixed with 1.0% (v/v) osmium tetraoxide and then stained with 1.0% (w/v) uranyl acetate. Tissues were dehydrated in ascending concentrations of ethanol prior to embedding in epoxy resin. Ultrathin sections were stained with uranyl acetate and lead citrate and examined with an Hitachi H-600 transmission electron microscope.

For scanning electron microscopy, tracheal tissues were fixed in 2.5% (v/v) glutaraldehyde in 0.1 M sodium cacodylate and postfixed using the osmium-thiocarbohydrazide-osmium (OTO) method (Kelly et al., 1973). Samples were dehydrated in ascending concentrations of ethanol and critical point dried in liquid CO_2. Mounted samples were sputter-coated with 50 nm of gold and examined with an Hitachi H-450 scanning electron microscope.

For immunoelectron microscopy, adult mouse tracheas were fixed in 4.0% (w/v) paraformaldehyde at 4°C for 2 hours. Tissue was dehydrated and embedded in glycol methacrylate resin. Sections were cut and incubated with rabbit polyclonal anti-human ezrin antibody (Upstate Biotechnology) at a dilution of 1:50. Sections were then incubated with a 10 nm gold-labeled goat anti-rabbit IgG secondary antibody, counterstained with uranyl acetate and examined with a JEOL-1200X transmission electron microscope. Duplicate samples were examined for transmission, scanning and immunoelectron microscopy.

Tracheal explant culture

For calpain inhibitor experiments, E17.5 *foxj1*$^{+/+}$ or *foxj1*$^{-/-}$ explanted mouse tracheas were cultured at air-liquid interface in the presence or absence of 10 mM calpain inhibitor II (N-acetyl-Leu-Leu-Met-al; Sigma) in BEGM serum-free medium (Clonetics) for 96 hours at 37°C in 5% CO_2. Tracheas were fixed in 3% glutaraldehyde/4% paraformaldehyde in 0.1 M sodium cacodylate for 2 hours and then washed in phosphate-buffered saline. Scanning electron microscopy and transmission electron microscopy were performed in duplicate as described above. For immunofluorescence, duplicate *foxj1*$^{+/+}$ and *foxj1*$^{-/-}$ explanted tracheas were fixed in 10% (v/v) buffered formalin and processed as above.

Results

Calpastatin is decreased in the pulmonary epithelium in the absence of Foxj1

To define the role of Foxj1 in cilia formation, DNA microarray analysis was performed to identify genes differentially expressed in *foxj1*$^{+/+}$ and *foxj1*$^{-/-}$ lung. 9+2 cilia are first detected in the mouse pulmonary epithelium at about E15.5 so this time point was selected for comparison. Total RNA from E15.5 *foxj1*$^{+/+}$ and *foxj1*$^{-/-}$ lung tissue was labeled and used to probe Affymetrix Mu74A microarrays. The absence of *foxj1* expression in homozygous mutant tissue was confirmed by RT-PCR using Foxj1-specific primers (data not shown). Microarray analysis was performed in triplicate with duplicate pooled samples of *foxj1*$^{+/+}$ and *foxj1*$^{-/-}$ RNA. The Mu74A microarrays are printed with approximately 16,000 mouse genes, including 12,000 known genes and 4,000 expressed sequence tags. Among the several genes that demonstrated consistent changes in expression in all three comparisons, the gene for calpastatin was identified as having two- to three-fold decreased expression in *foxj1*$^{-/-}$ versus *foxj1*$^{+/+}$ lung tissue. Because the *foxj1*$^{-/-}$ phenotype suggests a potential defect in basal body anchoring to the cytoskeleton and the role of calpastatin in cytoskeleton remodeling, we focused our initial studies on calpastatin. To confirm the decreased expression of calpastatin, RNase protection assays were performed. A 25-30% decrease in calpastatin transcript was consistently identified in E15.5 *foxj1*$^{-/-}$ lung tissue compared to E15.5 *foxj1*$^{+/+}$ lung tissue (Fig. 1A).

To further confirm the decrease in calpastatin, western blot analysis of protein from E15.5 *foxj1*$^{+/+}$, *foxj1*$^{+/-}$, and *foxj1*$^{-/-}$ lung tissue was performed using a primary antibody to calpastatin. An approximately 110 kDa protein and a 70 kDa protein were detected (Fig. 1B). The 110 kDa band represents full-length calpastatin, while the 70 kDa band represents a truncated form of calpastatin found in erythrocytes (Takano et al., 2000). A 50% decrease in the 110 kDa calpastatin protein was detected in *foxj1*$^{-/-}$ lung tissue and a 25% decrease was detected in the *foxj1*$^{+/-}$ lung

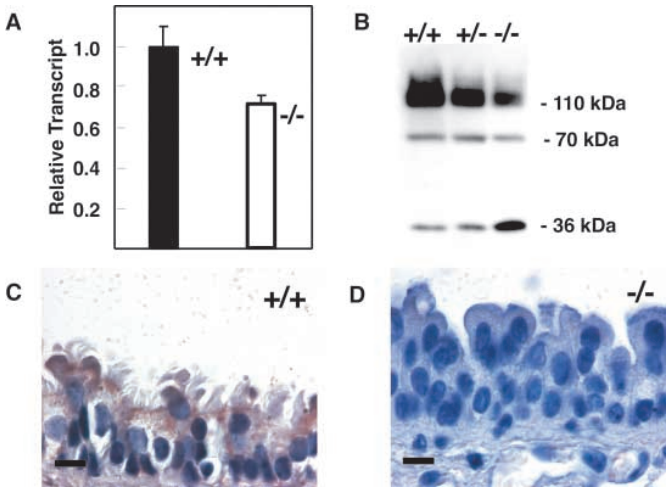

Fig. 1. Calpastatin is decreased in the absence of Foxj1. (A) RNase protection of E15.5 lung RNA with a [^{32}P]cRNA probe for calpastatin. Relative transcript abundance is shown in comparison with wild-type lung tissue (± s.e.m.). Samples were corrected for loading by comparison with GAPDH transcript abundance. (B) Western blot of E15.5 lung tissue with calpastatin primary antibody. Full-length tissue calpastatin is a 110 kDa protein and a truncated erythrocyte calpastatin isoform is a 70 kDa protein. GAPDH (36 kDa) abundance was used as a protein loading control. (C,D) Immunohistochemistry of *foxj1*$^{+/+}$ (C) and *foxj1*$^{-/-}$ (D) lung tissue with primary antibody to calpastatin and peroxidase detection. Scale bar: 5 μm.

tissue compared to E15.5 wild-type lung tissue (Fig. 1B). The 70 kDa protein reflects the number of residual erythrocytes present in a particular sample and thus may vary from sample to sample.

To examine the cell-specific pattern of decreased calpastatin in lung tissue from *foxj1*$^{-/-}$ mice, immunohistochemistry was performed with primary antibody to calpastatin. Expression of the *foxj1* gene is specific to ciliated cells of the pulmonary epithelium so it was expected that decreased calpastatin would be detected in the proximal pulmonary epithelium of *foxj1*$^{-/-}$ mice (Blatt et al., 1999; Hackett et al., 1995; Tichelaar et al., 1999). In *foxj1*$^{+/+}$ trachea, prominent peroxidase staining for calpastatin was noted throughout the epithelium (Fig. 1C). In comparison, there was a marked decrease in peroxidase staining for calpastatin in *foxj1*$^{-/-}$ tracheal epithelium (Fig. 1D). Thus, in the absence of Foxj1, there is less calpastatin protein present in the proximal pulmonary epithelium. No peroxidase staining was observed in the absence of primary calpastatin antibody (data not shown).

Calpain 2 is unchanged in the pulmonary epithelium in the absence of Foxj1

Calpastatin is a specific endogenous inhibitor of members of the calpain protease family (Sorimachi et al., 1997). Calpain 2 (or m-calpain) is the primary calpain isoform present in lung tissue (Beer et al., 1984; Thompson and Goll, 2000). Calpain 2 is active at millimolar concentrations of Ca^{2+} whereas the other ubiquitously expressed isoform, calpain 1 (or μ-calpain), is active at micromolar concentrations of Ca^{2+}. In addition to these widely distributed calpain isoforms, a number of tissue-specific isoforms have also been identified (Sorimachi et al., 1997). From western blot analysis with primary antibody to calpain 2, there is no significant change in calpain 2 protein levels in the lungs of *foxj1*$^{+/-}$ or *foxj1*$^{-/-}$ mice compared to wild-type mice (Fig. 2A). Additionally, from immunohistochemistry, there is no detectable change in calpain 2 protein in the proximal pulmonary epithelium of *foxj1*$^{-/-}$ mice compared to *foxj1*$^{+/+}$ mice (Fig. 2B,C). No staining was observed in the absence of primary calpain 2 antibody (data not shown).

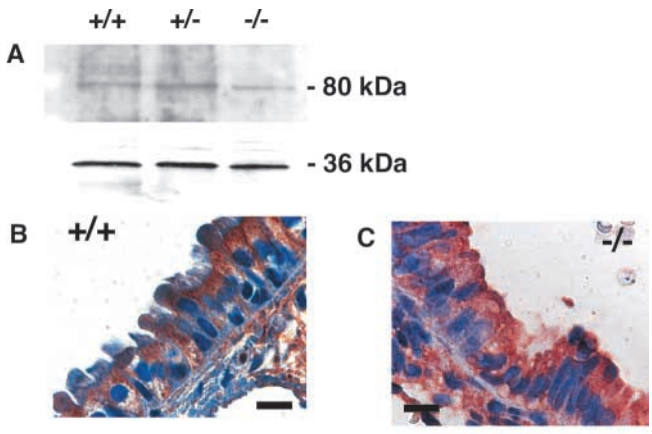

Fig. 2. No change in calpain 2 in the absence of Foxj1. (A) Western blot of E15.5 lung tissue with primary antibody to calpain 2. Calpain 2 is an 80 kDa protein. Comparison was made to GAPDH (36 kDa) to correct for protein loading. (B,C) Immunohistochemistry of *foxj1*$^{+/+}$ (B) and *foxj1*$^{-/-}$ (C) lung tissue with primary antibody to calpain 2 and peroxidase detection. Scale bar: 5 μm.

Ezrin is decreased in the pulmonary epithelium in the absence of Foxj1

The decrease in calpastatin in the proximal pulmonary epithelium of *foxj1*$^{-/-}$ mice suggests increased calpain proteolysis of cytoskeletal components as a possible mechanism for the mislocalization of basal bodies in this tissue. One of the cytoskeletal proteins sensitive to calpain proteolysis is the linking protein ezrin (Yao et al., 1993). Ezrin is an 80/81 kDa protein originally described as a substrate for receptor protein tyrosine kinases (Crepaldi et al., 1997; Gould et al., 1986). Ezrin acts as a linker molecule between the F-actin cytoskeleton and specific apical membrane proteins (Bretscher et al., 2002). By sequential, double immunofluorescence with primary antibody to ezrin and to acetylated α-tubulin, a specific marker for ciliated epithelial cells, ezrin was localized to the apices of ciliated epithelial cells in wild-type airway epithelium (Fig. 3C).

Western blot analysis detected a 40-50% decrease in the amount of ezrin protein in the lungs of *foxj1*$^{-/-}$ mice compared to wild-type mice (Fig. 3A). No significant decrease in ezrin protein was detected by western blot analysis in *foxj1*$^{+/-}$ mice, which have a normal phenotype, compared to wild-type mice (Fig. 3A). No change in ezrin gene transcription was detected by RT-PCR in the lungs of *foxj1*$^{-/-}$ mice compared to *foxj1*$^{+/+}$ lungs (Fig. 3B). Immunofluorescence with primary antibody to ezrin demonstrated a marked decrease in ezrin protein in the proximal pulmonary epithelium of *foxj1*$^{-/-}$ mice over that of

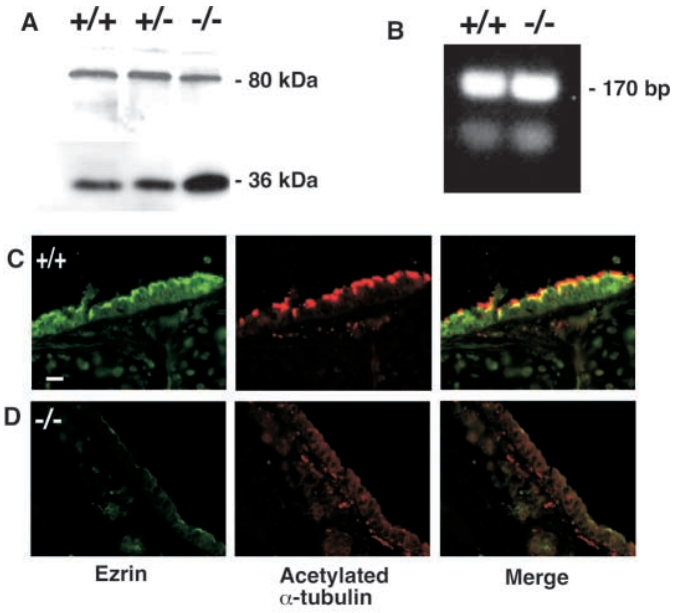

Fig. 3. Ezrin is decreased in the absence of Foxj1. (A) Western blot of E15.5 lung tissue with primary antibody to ezrin. Ezrin is an 80/81 kDa protein. Comparison was made to GAPDH (36 kDa) to correct for protein loading. (B) RT-PCR for ezrin expression in E15.5 lung tissue. A 170 bp ezrin product is detected in both *foxj1*$^{+/+}$ and *foxj1*$^{-/-}$ lung tissue. (C,D) Immunofluorescence of *foxj1*$^{+/+}$ (C) and *foxj1*$^{-/-}$ (D) in mouse trachea with primary antibody to ezrin or acetylated α-tubulin and detection of fluorescence. Scale bar: 10 μm.

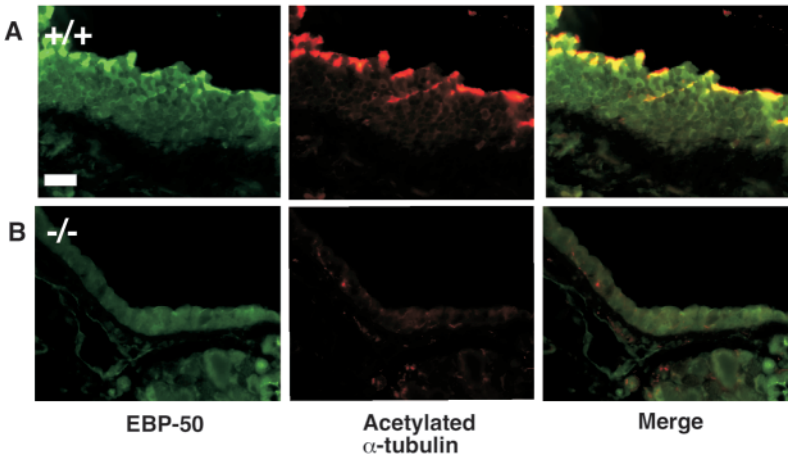

Fig. 4. EBP-50 is decreased in the absence of Foxj1. (A,B) Immunofluorescence of *foxj1*$^{+/+}$ (A) and *foxj1*$^{-/-}$ (B) in mouse trachea with primary antibody to EBP-50 or acetylated α-tubulin and fluorescence detection. Scale bar: 20 μm.

foxj1$^{+/+}$ mice (Fig. 3C,D). No fluorescent staining was observed in the absence of primary antibody (data not shown).

EBP-50 is decreased in the pulmonary epithelium in the absence of Foxj1

Ezrin binds to apical proteins either directly or indirectly through other scaffold proteins such as ezrin binding phosphoprotein 50 (EBP-50) or E3KARP (Bretscher et al., 2002). EBP-50 is a two PDZ-domain containing protein that links ezrin with apical proteins such as the cystic fibrosis transmembrane conductance regulator, the β_2-adrenergic receptor, the platelet-derived growth factor receptor and NHE-3 (Bretscher et al., 2002). By sequential, double immunofluorescence with primary antibody to EBP-50 and acetylated α-tubulin, EBP-50 was found to be localized to the apical region of ciliated cells in *foxj1*$^{+/+}$ airway epithelium in a fashion similar to ezrin (Fig. 4A). There was a marked decrease in EBP-50 observed in the airways of *foxj1*$^{-/-}$ mice compared to wild-type pulmonary epithelium (Fig. 4A,B).

Ezrin is associated with the basal bodies of ciliated epithelial cells

The decrease in ezrin in the proximal pulmonary epithelium in the absence of Foxj1 suggests a requirement for ezrin in anchoring of basal bodies to the apical cytoskeleton. Ezrin, as well as the related proteins moesin and radixin, participates in the anchoring of a variety of proteins to the apical cytoskeleton (Bretscher et al., 2002). In order to examine the relationship between ezrin and basal bodies in ciliated epithelial cells, immunoelectron microscopy was performed with primary ezrin antibody and gold-labeled secondary antibody. As demonstrated by western blot analysis, the primary ezrin antibody interacts with a single 80/81 kDa protein (Fig. 3A). In wild-type mouse trachea, ezrin was associated with basal bodies throughout the apical region of ciliated cells (Fig. 5A). No significant gold labeling was seen associated with axonemal structures or within the cytoplasm. As previously described for other epithelial cell types, ezrin was also noted to be associated with the microvilli of ciliated epithelial cells (Fig. 5A) (Berryman et al., 1993). No gold labeling was detected in the absence of primary ezrin antibody (Fig. 5B). In a trachea from a *foxj1*$^{-/-}$ mouse, as has been previously described, basal bodies were distributed throughout the cytoplasm of epithelial cells (Fig. 5C) (Brody et al., 2000). Additionally, microvilli appeared significantly flattened and nearly absent (Fig. 5C). By immunogold electron microscopy, no ezrin labeling was detected in association with basal bodies or microvilli in the absence of Foxj1 (Fig. 5C).

Calpain inhibition partially reverses the phenotype of absence of cilia in *foxj1*$^{-/-}$ mice

By scanning electron microscopy, explanted E17.5 wild-type mouse tracheas cultured at air-liquid interface for 96 hours demonstrated nearly 20% of the proximal pulmonary epithelial

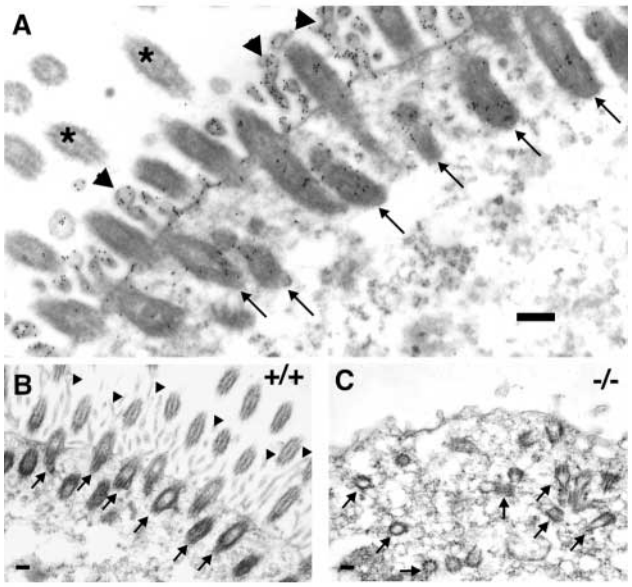

Fig. 5. Ezrin is associated with the basal bodies of ciliated epithelial cells. (A) Immunoelectron microscopy of tracheal epithelium with primary antibody for ezrin demonstrates gold particles associated with basal bodies (arrows) at the cell apex. Gold particles are also associated with the apical microvilli (arrowheads). No significant gold particles are seen in association with axonemal structures (*). Scale bar: 250 nm. (B) Transmission electron microscopy of trachea from a *foxj1*$^{+/+}$ mouse incubated with secondary gold-labeled antibody only. Microvilli (arrowheads) extend from the cell apex between axonemes. Basal bodies are localized at the cell apex (arrows). (C) Transmission electron microscopy of trachea from a *foxj1*$^{-/-}$ mouse incubated with primary antibody for ezrin and secondary gold-labeled antibody. No gold particles are detected in association with basal bodies that are distributed throughout the cytoplasm (arrows). No gold particles are associated with the microvilli that are severely flattened. No axonemal structures are present. Scale bar: 200 nm (B,C).

cells to be ciliated with abundant cilia noted on each cell (Table 1; Fig. 6A,D). Treatment of wild-type tracheal explants with 10 mM calpain inhibitor II for 96 hours did not significantly alter the number of ciliated cells or the density of cilia per cell (data not shown). In untreated, explanted *foxj1*$^{-/-}$ tracheas cultured for 96 hours, no 9+2 ciliated epithelial cells were observed (Table 1; Fig. 6B,E). 9+0 monocilia, or primary cilia, were observed throughout the untreated, explanted and cultured *foxj1*$^{-/-}$ tracheas (Fig. 6B). Treatment of explanted *foxj1*$^{-/-}$ tracheas with 10 mM calpain inhibitor II for 96 hours resulted in partial reversal of the *foxj1*$^{-/-}$ phenotype with the appearance of axonemal structures on some of the proximal pulmonary epithelial cells (Fig. 6C,F). The number of ciliated cells observed was about 4.1% of the total number of pulmonary epithelial cells (Table 1). These ciliated cells had fewer cilia per cell than the untreated or treated *foxj1*$^{+/+}$ ciliated cells (Fig. 6D, data not shown).

Table 1. Cilia recovery in *foxj1*$^{-/-}$ trachea following treatment with calpain inhibitor

Genotype	Calpain inhibitor II	Total cells	Ciliated Cells (%)
+/+	–	409	78 (19.1)
–/–	–	598	0 (0.0)
–/–	+	687	29 (4.1)

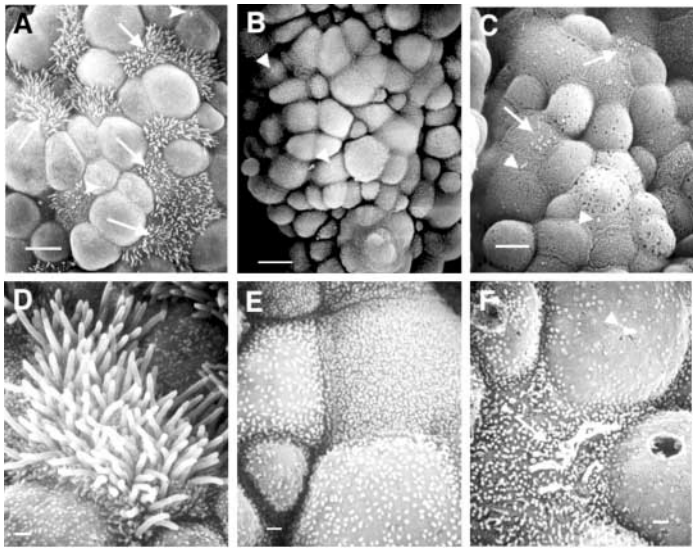

Fig. 6. Partial reversal of the *foxj1*$^{-/-}$ phenotype of no cilia with calpain inhibitor II treatment. Images D, E, F show higher magnification of A, B, C, respectively. (A,D) By scanning electron microscopy, multiple ciliated cells are observed in explanted E17.5 *foxj1*$^{+/+}$ trachea cultured for 96 hours (arrows). Cilia cover most of the apical cell surface. (B,E) By scanning electron microscopy, no 9+2 cilia are detected in explanted E17.5 *foxj1*$^{-/-}$ trachea cultured for 96 hours. 9+0 monocilia are observed (arrowheads). (C,F) Explanted *foxj1*$^{-/-}$ trachea cultured in the presence of 10 mM calpain inhibitor II for 96 hours demonstrates formation of cilia (arrows). The number of cilia per cell is less than in *foxj1*$^{+/+}$ trachea. 9+0 monocilia are also present (arrowheads). Scale bars: 5 μm (A-C); 500 nm (D-F).

Transmission electron microscopy of *foxj1*$^{+/+}$ tracheal explants demonstrated apical localization of basal bodies with axonemes extending into the lumen of the trachea (Fig. 7A). In the untreated *foxj1*$^{-/-}$ tracheal explants, basal bodies were observed throughout the cytoplasm with only rare individual basal bodies at the cell apex (Fig. 7B). In the *foxj1*$^{-/-}$ tracheal explants treated with 10 mM calpain inhibitor II, apical localization of basal bodies was observed (Fig. 7C).

The effect of calpain inhibition on the apical localization of ezrin and EBP-50 in *foxj1*$^{-/-}$ tracheal explants was examined by immunofluorescence (Fig. 8). Culture of *foxj1*$^{-/-}$ tracheal explants in the absence of calpain inhibitor II had no effect on the loss of apical ezrin or EBP-50 (Fig. 8A and data not shown). When *foxj1*$^{-/-}$ explants were cultured in the presence of 10 mM calpain II inhibitor, ezrin was detected in cell apices in association with acetylated α-tubulin, a marker for ciliated cells (Fig. 8B). In a similar fashion, treatment of explanted *foxj1*$^{-/-}$ tracheas resulted in a relocalization of EBP-50 to cell apices, also in association with acetylated α-tubulin (Fig. 8C). 10 mM calpain inhibitor II had no effect on localization of ezrin or EBP-50 in cultured, explanted wild-type tracheas (data not shown).

Discussion

Appropriate polarization of epithelial cells is essential to their many functions including ion and water transport, ligand-receptor interaction, exocytosis, and cell division. During cellular differentiation, epithelial cells become polarized with respect to their apical and basal surfaces through the interactions of junctional proteins with the cellular cytoskeleton (Wodarz, 2002). Localization of proteins to the apical or basal compartments of the cell requires mechanisms for segregating these proteins as well as maintaining the appropriate localization. Directional microtubule transport mediated by kinesin and dynein motor proteins is required for the initial segregation of proteins to the apical or basal compartment (Hirokawa, 1998). The cortical cytoskeleton provides a stable anchoring point for proteins localized to the apical cell compartment. Proteins such as the cystic fibrosis

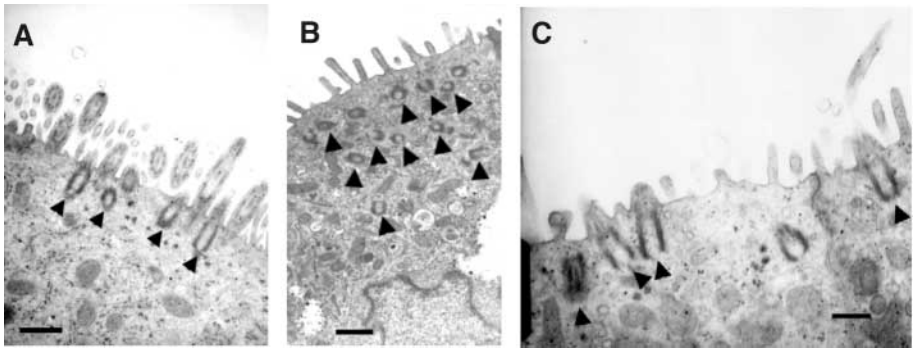

Fig. 7. Calpain inhibition results in apical relocalization of basal bodies in *foxj1*$^{-/-}$ trachea. (A,B) By transmission electron microscopy, basal bodies (arrowheads) are found to be apically localized in an E17.5 *foxj1*$^{+/+}$ tracheal explant (A), but distributed throughout the cytoplasm of *foxj1*$^{-/-}$ tracheal explant (B); both cultured for 96 hours. (C) Treatment of cultured E17.5 *foxj1*$^{-/-}$ tracheal explant with 10 mM calpain II inhibitor results in localization of basal bodies (arrowheads) to cell apex. Scale bars: 500 nm (A,B); 250 nm (C).

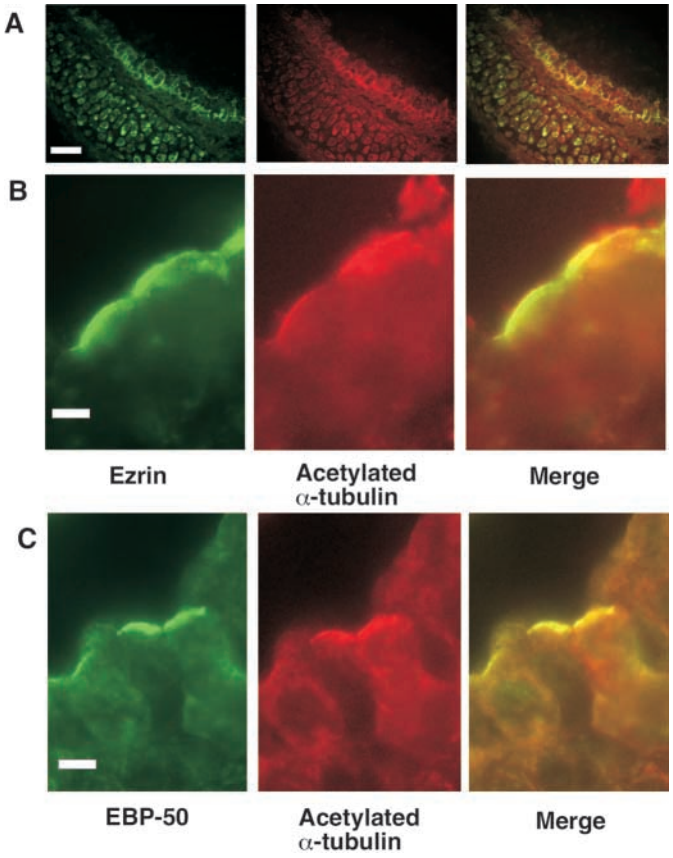

Fig. 8. Calpain inhibition results in apical localization of ezrin and EBP-50 in *foxj1*$^{-/-}$ trachea. (A) Immunofluorescence of untreated, E17.5 *foxj1*$^{-/-}$ tracheal explant cultured for 96 hours with primary antibody to ezrin and acetylated α-tubulin. (B) Immunofluorescence of E17.5 *foxj1*$^{-/-}$ tracheal explant cultured for 96 hours in the presence of 10 mM calpain inhibitor II with primary antibody to ezrin and acetylated α-tubulin. (C) Immunofluorescence of E17.5 *foxj1*$^{-/-}$ tracheal explant cultured for 96 hours in the presence of 10 mM calpain inhibitor II with primary antibody to EBP-50 and acetylated α-tubulin. Scale bars: 20 μm (A); 2.5 μm (B); 5 μm (C).

transmembrane conductance regulator are linked to the cortical cytoskeleton through protein-protein interactions (Short et al., 1998). The axonemes of ciliated epithelial cells also require appropriate localization to the cell apex for proper function. Anchoring of basal bodies to the cortical cytoskeleton would provide a mechanism for the appropriate apical localization of axonemes.

Targeted mutation of the mouse *foxj1* gene provides new insight into the mechanisms regulating the apical anchoring of basal bodies and axonemes. In the absence of Foxj1, axonemal structures do not form and basal bodies are found throughout the cytoplasm of cells instead of in the apical compartment (Brody et al., 2000; Chen et al., 1998). By microarray analysis of embryonic lung tissue from *foxj1*$^{+/+}$ and *foxj1*$^{-/-}$ mice, the calpastatin gene has been identified as one of the genes with decreased expression in the absence of Foxj1. Calpastatin is a specific endogenous inhibitor of the protease calpain and acts by binding to calpain (Sorimachi et al., 1997). The balance between calpain proteolysis and calpastatin inhibition regulates stability of the cytoskeleton in a variety of circumstances (Barnoy et al., 1998; Barnoy et al., 2000; Croce et al., 1999; Dwyer-Nield et al., 1996; Potter et al., 1998). Calpastatin and the various calpain isoforms are ubiquitous proteins present in a wide range of cell types. Because the requirements for cytoskeletal stability may vary from cell type to cell type, cell-specific mechanisms of regulation of calpain activity would be required to meet the specific needs of each cell type. Cell-specific regulation of calpastatin gene expression by Foxj1 in ciliated cells would provide such a mechanism. In the absence of Foxj1, a decrease in calpastatin protein in the proximal pulmonary epithelium, without any significant change in calpain protein levels, would result in increased calpain proteolytic activity. Partial reversal of the *foxj1*$^{-/-}$ phenotype with a calpain inhibitor is consistent with increased calpain proteolytic activity resulting in the loss of basal body anchoring in the absence of Foxj1. It cannot be determined from the current data whether the calpastatin gene is a direct or indirect target of regulation by Foxj1. Examination of over 5000 base pairs of the 5′-flanking region of the human calpastatin gene did not reveal any core Foxj1 binding sequences (TGTTTGT) (Lim et al., 1997). Further studies will be required to elucidate the mechanism of calpastatin gene regulation by Foxj1.

A number of cytoskeletal proteins have been identified as potential substrates for proteolysis by calpain. Calpain proteolysis of ezrin with associated cytoskeletal changes has been demonstrated in endothelial cells, lymphocytes, neutrophils, NIH-3T3 cells, renal proximal tubule cells and gastric parietal cells (Aono et al., 2001; Ariyoshi et al., 2001; Chen et al., 1994; Potter et al., 1998; Shcherbina et al., 1999; Yao et al., 1993). Ezrin co-localized with acetylated α-tubulin, a marker of ciliated cells, in the pulmonary epithelium. Additionally, ezrin was found, by immunoelectron microscopy, to be associated with the basal bodies of ciliated cells. In the absence of Foxj1, ezrin is markedly reduced in the proximal pulmonary epithelium presumably as the result of increased calpain proteolysis and not because of decreased ezrin gene expression. Other calpain substrates may be similarly reduced in the absence of Foxj1. Linkage of apical proteins to the cytoskeleton by ezrin may involve a second PDZ-domain protein, EBP-50. Co-localization studies with acetylated α-tubulin indicate that EBP-50 is also associated with the apical compartment of ciliated epithelial cells. Although EBP-50 has not been demonstrated to be a substrate for calpain proteolysis, it was also reduced in the proximal pulmonary epithelium in the absence of Foxj1. The decrease in EBP-50 may be a result of increased turnover of EBP-50 or redistribution of the protein in response to changes in the cytoskeleton. Additionally, both ezrin and EBP-50 relocalize to the apical cell compartment following treatment of *foxj1*$^{-/-}$ tracheas with a calpain inhibitor suggesting a role for these proteins in anchoring basal bodies to the apical cytoskeleton.

Foxj1 thus maintains cytoskeletal stability in ciliated cells by maintaining calpastatin gene expression and inhibiting subsequent calpain proteolysis of ezrin or possibly other cytoskeletal elements. As demonstrated here, ezrin is associated with the basal bodies of ciliated pulmonary epithelial cells providing a potential mechanism for linking basal bodies to the apical cytoskeleton. In the absence of Foxj1, there is a loss of ezrin and EBP-50 from the proximal

pulmonary epithelium and an associated failure of appropriate basal body localization and axoneme formation. Also, not surprisingly, given the role of ezrin in microvillar structure, the microvilli of tracheal epithelial cells are abnormal in *foxj1*$^{-/-}$ mice. This suggests that the loss of apical anchoring in the absence of Foxj1 may affect multiple apical components.

Breakdown and remodeling of the apical cytoskeleton play an important role in a number of developmental and physiological processes (Bretscher et al., 2002). At other times, however, stability of the cytoskeleton is necessary for normal cell function. By inhibiting the calpain-mediated proteolysis of cytoskeletal components, such as ezrin, calpastatin contributes to cytoskeleton stability (Aono et al., 2001; Ariyoshi et al., 2001; Chen et al., 1994; Potter et al., 1998; Shcherbina et al., 1999). Maintaining cytoskeleton stability would be essential to the normal differentiation of ciliated epithelial cells during lung development. In pulmonary diseases such as asthma, and certain lung infections, loss of cilia is an important component of defective mucociliary clearance (Salathe et al., 1997). For example, in paramyxoviral infection of the mouse airway epithelium there is a loss and subsequent recovery of cilia. This loss and recovery of cilia are accompanied by a decrease and subsequent increase in Foxj1 with recovery from infection (Look et al., 2001). Elucidating the mechanisms regulating basal body anchoring to the apical cytoskeleton may thus have important implications with respect to understanding pulmonary epithelial diseases and may suggest novel therapeutic approaches to them.

The authors wish to thank Wandy Beatty, Nancy Galvin and Mike Veith for technical assistance with electron microscopy and Min Zhang for thoughtful discussions. B.N.G. is an NICHD Fellow of the Pediatric Scientist Development Program (NICHD Grant Award K12-HD00850). B.P.H. is supported by NICHD R01 HD37036.

References

Afzelius, B. A. and Mossberg, B. (1995). Immotile-cilia syndrome (primary ciliary dyskinesia), including Kartagener syndrome. In *The Metabolic and Molecular Bases of Inherited Disease*, vol. III (ed. C. R. Scriver, A. L., Beaudet W. S. Sly and D. Valle), pp. 3943-3954. New York: McGraw-Hill.

Aono, Y., Ariyoshi, H., Tsuji, Y., Ueda, A., Tokunaga, M., Sakon, M. and Monden, M. (2001). Localized activation of m-calpain in human umbilical vein endothelial cells upon hypoxia. *Thromb. Res.* **102**, 353-361.

Ariyoshi, H., Yoshikawa, N., Aono, Y., Tsuji, Y., Ueda, A., Tokunaga, M., Sakon, M. and Monden, M. (2001). Localized activation of m-calpain in migrating human umbilical vein endothelial cells stimulated by shear stress. *J. Cell. Biochem.* **81**, 184-192.

Barnoy, S., Glaser, T. and Kosower, N. S. (1998). The calpain-calpastatin system and protein degradation in fusing myoblasts. *Biochim. Biophys. Acta* **1402**, 52-60.

Barnoy, S., Supino-Rosin, L. and Kosower, N. S. (2000). Regulation of calpain and calpastatin in differentiating myoblasts: mRNA levels, protein synthesis and stability. *Biochem. J.* **351**, 413-420.

Beer, D. G., Butley, M. S. and Malkinson, A. M. (1984). Developmental changes in the endogenous Ca^{2+}-stimulated proteolysis of mouse lung cAMP-dependent protein kinases. *Arch. Biochem. Biophys.* **288**, 207-219.

Berryman, M., Franck, Z. and Bretscher, A. (1993). Ezrin is concentrated in the apical microvilli of a wide variety of epithelial cells whereas moesin is found primarily in endothelial cells. *J. Cell Sci.* **105**, 1025-1043.

Blatt, E. N., Yan, X. H., Wuerffel, M. K., Hamilos, D. L. and Brody, S. L. (1999). Forkhead transcription factor HFH-4 expression is temporally related to ciliogenesis. *Am. J. Respir. Cell Mol. Biol.* **21**, 168-176.

Bretscher, A., Edwards, K. and Fehon, R. G. (2002). ERM proteins and merlin: integrators at the cell cortex. *Nat. Rev. Mol. Cell. Biol.* **3**, 586-599.

Brody, S. L., Yan, X. H., Wuerffel, M. K., Song, S.-K. and Shapiro, S. D. (2000). Ciliogenesis and left-right axis defects in forkhead factor HFH-4-null mice. *Am. J. Respir. Cell Mol. Biol.* **23**, 45-51.

Chen, J., Doctor, R. B. and Mandel, L. J. (1994). Cytoskeletal dissociation of ezrin during renal anoxia: role in microvillar injury. *Am. J. Physiol.* **267**, C784-C795.

Chen, J., Knowles, H. J., Hebert, J. L. and Hackett, B. P. (1998). Mutation of the mouse hepatocyte nuclear factor/forkhead homologue 4 gene results in an absence of cilia and random left-right asymmetry. *J. Clin. Invest.* **102**, 1077-1082.

Cole, D. G., Diener, D. R., Himelblau, A. L., Beech, P. L., Fuster, J. C. and Rosenbaum, J. L. (1998). *Chlamydomonas* kinesin-II-dependent intraflagellar transport (IFT): IFT particles contain proteins required for ciliary assembly in *Caenorhabditis elegans* sensory neurons. *J. Cell Biol.* **141**, 993-1008.

Crepaldi, T., Gautreau, A., Comoglio, P. M., Louvard, D. and Arpin, M. (1997). Ezrin is an effector of hepatocyte growth factor-mediated migration and morphogenesis in epithelial cells. *J. Cell Biol.* **138**, 423-434.

Croce, K., Flaumenhauft, R., Rivers, M., Furie, B., Furie, B. C., Herman, I. M. and Potter, D. A. (1999). Inhibition of calpain blocks platelet secretion, aggregation, and spreading. *J. Biol. Chem.* **274**, 36321-36327.

Dirksen, E. R. (1991). Centriole and basal body formation during ciliogenesis revisited. *Biol. Cell* **72**, 31-38.

Dutcher, S. K. (1995). Flagellar assembly in two hundred and fifty easy-to-follow steps. *Trends Genet.* **11**, 398-404.

Dwyer-Nield, L. D., Miller, A. C. K., Neighbors, B. W., Dinsdale, D. and Malkinson, A. M. (1996). Cytoskeletal architecture in mouse lung epithelial cells is regulated by protein kinase C-α and calpain II. *Am. J. Physiol.* **270**, L526-L534.

Geimer, S., Clees, J., Melkonian, M. and Lechtreck, K.-F. (1998). A novel 95-kD protein is located in a linker between cytoplasmic microtubules and basal bodies in a green flagellate and forms striated filaments in vitro. *J. Cell Biol.* **140**, 1149-1158.

Gould, K. L., Cooper, J. A., Bretscher, A. and Hunter, T. (1986). The protein-tyrosine kinase substrate, p81, is homologous to a chicken microvillar core protein. *J. Cell Biol.* **102**, 660-669.

Guichard, C., Harricane, M.-C., Lafitte, J.-J., Godard, P., Zaegal, M., Tack, V., Lalau, G. and Bouvagnet, P. (2001). Axonemal dynein intermediate-chain gene (DNAI1) mutations result in situs inversus and primary ciliary dyskinesia (Kartagener syndrome). *Am. J. Hum. Genet.* **68**, 1030-1035.

Hackett, B. P., Brody, S. L., Liang, M., Zeitz, I. D., Bruns, L. A. and Gitlin, J. D. (1995). Primary structure of hepatocyte nuclear factor/forkhead homologue 4 and characterization of gene expression in developing respiratory and reproductive epithelium. *Proc. Natl. Acad. Sci. USA* **92**, 4249-4253.

Hirokawa, N. (1998). Kinesin and dynein superfamily and the mechanism of organelle transport. *Science* **279**, 519-526.

Kelly, R. O., Dekker, R. A. and Bluemink, J. G. (1973). Ligand-mediated osmium binding: its application in coating biological specimens for scanning electron microscopy. *J. Ultrastruct. Res.* **45**, 254-258.

Knowles, M. R. and Boucher, R. C. (2002). Mucus clearance as a primary innate defense mechanism for mammalian airways. *J. Clin. Invest.* **109**, 571-577.

Lechtreck, K.-F., Teltenkotter, A. and Grunow, A. (1999). A 210 kDa protein is located in a membrane-microtubule linker at the distal end of mature and nascent basal bodies. *J. Cell Sci.* **112**, 1633-1644.

Lim, L., Zhou, H. and Costa, R. H. (1997). The winged helix transcription factor HFH-4 is expressed during choroid plexus epithelial development in mouse embryo. *Proc. Natl. Acad. Sci. USA* **94**, 3094-3099.

Look, D. C., Walter, M. J., Williamson, M. R., Pang, L., You, Y., Sreshta, J. N., Johnson, J. E., Zander, D. S. and Brody, S. L. (2001). Effects of paramyxoviral infection on airway epithelial cell Foxj1 expression, ciliogenesis, and mucociliary function. *Am. J. Pathol.* **159**, 2055-2069.

Marszalek, J. R., Ruiz-Lozano, P., Roberts, E., Chien, K. and Goldstein, L. S. B. (1999). Situs inversus and embryonic ciliary morphogenesis defects in mouse mutants lacking the KIF3A subunit of kinesin II. *Proc. Natl. Acad. Sci. USA* **96**, 5043-5048.

Nonaka, S., Tanaka, Y., Okada, Y., Takeda, S., Harada, A., Kanai, Y., Kido, M. and Hirokawa, N. (1998). Randomization of left-right asymmetry due to loss of nodal cilia generating leftward flow of extraembryonic fluid in mice lacking KIF3B motor protein. *Cell* **95**, 829-837.

Olbrich, H., Haffner, K., Kispert, A., Volkel, A., Volz, A., Sasmaz, G., Reinhardt, R., Hennig, S., Lehrach, H., Konietzko, N. et al. (2002).

Mutations in DNAH5 cause primary ciliary dyskinesia and randomization of left-right asymmetry. *Nat. Genet.* **30**, 143-144.

Pelletier, G. J., Brody, S. L., Liapis, H., White, R. A. and Hackett, B. P. (1998). A human forkhead/winged helix transcription factor expressed in developing pulmonary and renal epithelium. *Am. J. Physiol.* **274**, L351-L359.

Pennarun, G., Escudier, E., Chapelin, C., Bridoux, A.-M., Cacheux, V., Roger, G., Clement, A., Goossens, M., Amselm, S. and Duriez, B. (1999). Loss-of-function mutations in a human gene related to Chlamydomonas reinhardtii dynein IC78 result in primary ciliary dyskinesia. *Am. J. Hum. Genet.* **65**, 1508-1519.

Potter, D. A., Tirnauer, J. S., Janssen, R., Croall, D. E., Hughes, C. N., Fiacco, K. A., Mier, J. W., Maki, M. and Herman, I. M. (1998). Calpain regulates actin remodeling during cell spreading. *J. Cell Biol.* **141**, 647-662.

Preble, A. M., Giddings, J. T. M. and Dutcher, S. K. (2000). Basal bodies and centrioles: their function and structure. *Curr. Top. Dev. Biol.* **49**, 207-233.

Salathe, M., O'Riordan, T. G. and Wanner, A. (1997). Mucociliary clearance. In *The Lung Scientific Foundations*, vol. 2 (ed. R. G. Crystal, J. B. West, E. R. Weibel and P. J. Barnes), pp. 2295-2308. Philadelphia: Lippincott-Raven.

Shcherbina, A., Bretscher, A., Kenny, D. M. and Remold-O'Donnell, E. (1999). Moesin, the major ERM protein of lymphocytes and platelets, differs from ezrin in its insensitivity to calpain. *FEBS Lett.* **443**, 31-36.

Short, D. B., Trotter, K. W., Reczek, D., Kreda, S. M., Bretscher, A., Boucher, R. C., Stutts, M. J. and Milgram, S. L. (1998). An apical PDZ protein anchors the cystic fibrosis transmembrane conductance regulator to the cytoskeleton. *J. Biol. Chem.* **273**, 19797-19801.

Silflow, C. D., LaVoie, M., Tam, L. W., Tousey, S., Sanders, M., Wu, W.-C., Borodovsky, M. and Lefebvre, P. A. (2001). The Vfl1 protein in *Chlamydomonas* localizes in a rotationally asymmetric pattern at the distal ends of the basal bodies. *J. Cell Biol.* **153**, 63-74.

Sorimachi, H., Ishiura, S. and Suzuki, K. (1997). Structure and physiological function of calpains. *Biochem. J.* **328**, 721-732.

Sorokin, S. P. (1968). Reconstruction of centriole formation and ciliogenesis in mammalian lungs. *J. Cell Sci.* **3**, 207-230.

Takano, J., Watanabe, M., Hitomi, K. and Maki, M. (2000). Four types of calpastatin isoforms with distinct amino-terminal sequences are specified by alternative first exons and differentially expressed in mouse tissues. *J. Biochem.* **128**, 83-92.

Takeda, S., Yonekawa, Y., Tanaka, Y., Okada, Y., Nonaka, S. and Hirokawa, N. (1999). Left-right asymmetry and kinesin superfamily protein KIF3A: new insights in determination of laterality and mesoderm induction by *kif3A*$^{-/-}$ mice analysis. *J. Cell Biol.* **145**, 825-836.

Tam, L. W. and Lefebvre, P. A. (1993). Cloning of flagellar genes in *Chlamydomonas reinhardtii* by DNA insertional mutagenesis. *Genetics* **135**, 375-384.

Taulman, P. D., Haycraft, C. J., Balkovetz, D. F. and Yoder, B. K. (2001). Polaris, a protein involved in left-right axis patterning, localizes to basal bodies and cilia. *Mol. Biol. Cell* **12**, 589-599.

Thompson, V. F. and Goll, D. E. (2000). Purification of μ-calpain, m-calpain, and calpastatin from animal tissues. In *Calpain methods and protocols*, vol. 144 (ed. Elce, J. S.), pp. 3-16. Totowa, New Jersey: Humana Press.

Tichelaar, J. W., Wert, S. E., Costa, R. H., Kimura, s. and Whitsett, J. A. (1999). HNF-3/forkhead homologue-4 (HFH-4) is expressed in ciliated epithelial cells in the developing mouse lung. *J. Histochem. Cytochem.* **47**, 823-831.

Wodarz, A. (2002). Establishing cell polarity in development. *Nat. Cell Biol.* **4**, E39-E44.

Yao, X., Thibodeau, A. and Forte, J. G. (1993). Ezrin-calpain I interactions in gastric parietal cells. *Am. J. Physiol.* **265**, C36-C46.